Int. J. Solids Structures Vol. 30, No. 15, pp. 2009–2026, 1993
Printed in Great Britain

0020–7683/93 $6.00+ .00

SENSITIVITIES AND OPTIMAL DESIGN OF HEXAGONAL ARRAY FIBER COMPOSITES WITH RESPECT TO INTERPHASE PROPERTIES

SUNIL N. GULRAJANI and SUBRATA MUKHERJEE
Department of Theoretical and Applied Mechanics, Cornell University,
Ithaca, NY 14853, U.S.A.

(*Received* 25 *September* 1992; *in revised form* 28 *January* 1993)

Abstract—The focus of this paper is the calculation of sensitivities of stresses at an interphase between a fiber and matrix, in a hexagonal cell of a fiber-reinforced composite, with respect to interphase stiffnesses, and the use of these sensitivities to carry out optimal design of the interphase stiffnesses. The interphase is modeled here as a spring layer. Sensitivities are of interest in the design of composites since interphase properties can substantially affect the mechanical and thermal behavior of a composite. The sensitivity calculations are carried out here by using the direct differentiation approach (DDA) of the corresponding boundary element method (BEM) formulation of the problem. Optimization calculations are carried out by coupling the standard and sensitivity analyses to an optimizer. The optimizer chosen here uses sequential quadratic programming to obtain the desired optimal values of interphase stiffnesses that minimize the possibility of failure of a composite under prescribed loading.

Numerical results for sensitivities and optimization, for some illustrative examples, are presented in this paper.

1. INTRODUCTION

The focus of this paper is a study of the effect of interphases, between a fiber and a matrix in a composite material, on the stresses in the composite—both in the fiber and in the matrix. An interphase is a thin interfacial zone, between a fiber and a matrix, across which bonding between the two main phases of the composite takes place.

Interphase properties can substantially affect the mechanical and thermal behavior of a composite—both during a thermal curing cycle and during use of a composite structure. Such effects have been studied by several authors [e.g. Walpole (1978), Mikata and Taya (1985a, b) and Ochiai and Osamura (1987)]. In related studies, two analytical models have been considered. Broutman and Agarwal (1974), Theocaris *et al.* (1985), Maurer *et al.* (1986), Sideridis (1988), and Benveniste *et al.* (1989) have modeled the interphase as a thin layer between a fiber (or an inclusion) and a matrix, with specified thickness and elastic constants different from those of the fiber and the matrix. In reality, however, experimental determination of such interphase properties is very difficult. An alternative spring layer model has been employed by Lene and Leguillon (1982), Benveniste (1985), Aboudi (1987), Stief and Hoysan (1987), Hashin (1990, 1991), and Achenbach and Zhu (1989, 1990). In this model, it is assumed that the normal and tangential tractions are continuous across the interphase (in order to satisfy equilibrium), but the displacements can suffer discontinuities across the interphase. Such displacement jumps, when present, are proportional to their associated traction components, with the proportionality constants characterizing the stiffness of the interphase. The actual thickness of an interphase layer is left unspecified in this model. It should be mentioned here that Jasiuk and Tong (1989) have studied both the above models.

An interphase can be a by-product of manufacture or it might be deliberately introduced. A coating on the reinforcing fibers is a common example. In a recent paper, Shieu *et al.* (1990) have experimentally demonstrated that the shearing strength of a metal ceramic interphase (in this case for a NiO-Pt system) can be substantially increased by suitable heat treatment. Depending on the choice of annealing temperature, time and oxygen partial pressure, an interphase layer of either an intermetallic compound NiPt (of thickness between 1 and 65 nm) or a Ni-Pt solid solution can be produced. Compared to its originally hot-pressed state, the shearing strength of the NiO-Pt interface was increased by a factor of at

least four by the presence of the NiPt and by about 10 by the solid solution. This is remarkable considering the fact that the interphase layer is extremely thin in this case.

Studies such as the above by Shieu *et al.* (1990) raise intriguing questions and exciting possibilities. Is it possible, for example, to tailor composite interphase properties such as strength and stiffness to achieve desired objectives? A possible objective might be to minimize the maximum residual tensile stress in the matrix of a metal matrix composite following a thermal cycle. Such questions lie in the realm of inverse or design problems rather than merely simulation of composite systems. Optimization techniques are often useful for obtaining rational solutions of such problems.

An optimization process typically starts from a preliminary design and calculation of design sensitivity coefficients (DSCs) for this design. The DSCs are rates of change of response quantities such as stress or displacement in a loaded body, with respect to design variables. Design variables could be material parameters, boundary conditions or shape parameters that control the shape of the body. An optimization algorithm [e.g. Vanderplaats (1985)] uses nonlinear programming to start from the preliminary design and its sensitivities to propose a new design. The goal is to optimize an objective function without violating the constraints of a problem. This process is carried out in an iterative manner, producing a succession of designs, until an optimal design is obtained. While optimization problems for linear problems in continuum mechanics (e.g. linear elasticity) are fairly common, those for nonlinear problems (e.g. elasto-viscoplastic) have only recently begun to attract attention [e.g. Wei *et al.* (1993)].

The objective of this paper is to determine sensitivities of stresses in a composite material with respect to interphase stiffnesses and then use these sensitivities in an optimization procedure to obtain the optimal values of these stiffnesses in certain cases. Basically, three different approaches have been used in literature for the calculation of DSCs—the finite difference approach (FDA), the adjoint structure approach (ASA) and the direct differentiation approach (DDA). Also, both the finite element method (FEM) and the boundary element method (BEM) have been used for these analyses by different researchers. The FDA is the simplest approach and is based on the difference of two neighboring solutions of a problem, one for a nominal and the other for a slightly perturbed value of the design variable. This method, however, can be unreliable and should be used with caution. It is shown later in this paper that, under certain circumstances, the FDA can deliver totally erroneous results for DSCs for interphase tractions in composites, with respect to interphase stiffness.

Attention is now focused on a very promising approach for obtaining the DSCs—the DDA of the governing BEM equations of a problem. Here, the exact differentiation eliminates errors that might occur from using finite differences and leads to closed form integral equations for the desired sensitivities. These equations are then solved by numerical discretization. This approach is very accurate and efficient. It has been employed to obtain DSCs for linear elastic problems by various researchers, e.g. for planar (Barone and Yang, 1988; Kane and Saigal, 1988; Choi and Choi, 1990; Zhang and Mukherjee, 1991), axisymmetric (Saigal *et al.*, 1989; Rice and Mukherjee, 1990) and three-dimensional (Barone and Yang, 1989; Aithal *et al.*, 1991) problems. Sensitivities for materially nonlinear problems such as those involving elasto-viscoplasticity (Zhang *et al.*, 1992a) and for fully nonlinear problems such as large strain elasto-viscoplasticity (Zhang *et al.*, 1992b) have also been obtained using the DDA of the BEM equations.

On the optimization front, different methods, such as the steepest descent, quadratic programming, sequential quadratic programming, etc. (Haftka *et al.*, 1990) have been employed by different researchers. The plan in this work is to use the DSCs obtained above, with existing available optimization subroutines, to obtain illustrative optimal solutions.

The present work assumes a periodic configuration of fibers and calculations are carried out on a basic cell. This cell contains a single fiber with surrounding matrix, and its boundaries are subjected to appropriate tractions or displacements that are consistent with the periodic structure of the composite and the far field loading. Such calculations have been carried out for perfect bonds by Adams (1987) and Zywicz (1986) and for interphases modeled as spring layers, by Achenbach and Zhu (1989) for rectangular, and Achenbach

and Zhu (1990) for hexagonal arrays. Achenbach and Zhu (1989) found that variations of interphase parameters cause pronounced changes in the stress fields in the composite cell. For the hexagonal array, Achenbach and Zhu (1990) found that the maximum circumferential stress, along the matrix side of the interphase, is strongly dependent on the interphase stiffness and the fiber volume ratio.

The hexagonal array model, with an interphase in a unit cell described by a spring layer (Achenbach and Zhu, 1990), is the starting point of the present work. A basic cell of trapezoidal shape, subjected to a far-field uniform tensile stress in the closest packing direction (CPD) or in the mid-closest packing direction (mid-CPD) is analysed by the boundary element method (BEM). Next, sensitivities of stresses and displacements, with respect to the interphase stiffnesses in the radial and tangential directions, are obtained by using the DDA of the BEM. This approach follows that used earlier for isotropic linear elastic problems by Zhang and Mukherjee (1991). Isoparametric, quadratic boundary elements are employed for both the usual mechanics and the sensitivity problems in implementing the BEM.

The DDA of BEM results for the sensitivities are compared with those obtained from finite differences of two neighboring BEM solutions, and generally show good agreement. An interesting situation arises if the interphase configuration (defined by interphase nodes at which the matrix and the fiber are in physical contact, and nodes that are separated by the spring layer) undergoes a change due to a small increment in the stiffness. In such a situation, the sensitivities with respect to interphase stiffnesses suffer jump discontinuities. The present method (DDA of the BEM) delivers accurate solutions in such cases, whereas the FDA approach can produce totally erroneous results.

The sensitivities of stresses, calculated as described above, are used in this paper to carry out optimal design of the interphase stiffnesses for some examples. The central idea here is to design interphase stiffnesses to minimize the possibility of failure of the composite subjected to certain prescribed loading conditions. The optimization problems considered here are of the min-max type in which the maximum value of a tensile stress component, or a combination of these stress components, is minimized as a function of interphase stiffnesses. The sequential quadratic programming algorithm, due to Schittkowski (1986), available as the subroutine N0ONF, available as a part of the fortran IMSL subroutine library is used here to solve the optimization problems.

2. PROBLEM FORMULATION

Following Achenbach and Zhu (1990), Fig. 1 shows a periodic fiber reinforced composite with a unit hexagonal cell. The composite is subjected to a remote uniform stress σ_0 in the closest packing direction (CPD) which is labeled the global x direction. Each unit hexagonal cell has sides b and each fiber is of radius a. Due to periodicity and symmetry, only one quarter of the cell, $ABCD$ needs to be considered here. Figure 2 shows the situation for loading in the mid-CPD direction. Only the CPD direction is discussed below and the reader should refer to Achenbach and Zhu (1990) for details of the mid-CPD case.

With the origin at the mid-point O of the side DC (Fig. 1), the stress and displacement boundary conditions around the trapezoid are

$$AB: \quad \tau_1 = 0, \quad u_2 = C_2, \tag{1}$$

$$BC: \quad \tau_2 = 0, \quad u_1 = C_1/2, \tag{2}$$

$$DA: \quad \tau_2 = 0, \quad u_1 = -C_1/2, \tag{3}$$

$$DC: \quad \begin{cases} u_1(-x, -y) = -u_1(x, y), \\ u_2(-x, -y) = -u_2(x, y), \\ \tau_1(-x, -y) = \tau_1(x, y), \\ \tau_2(-x, -y) = \tau_2(x, y), \end{cases} \tag{4}$$

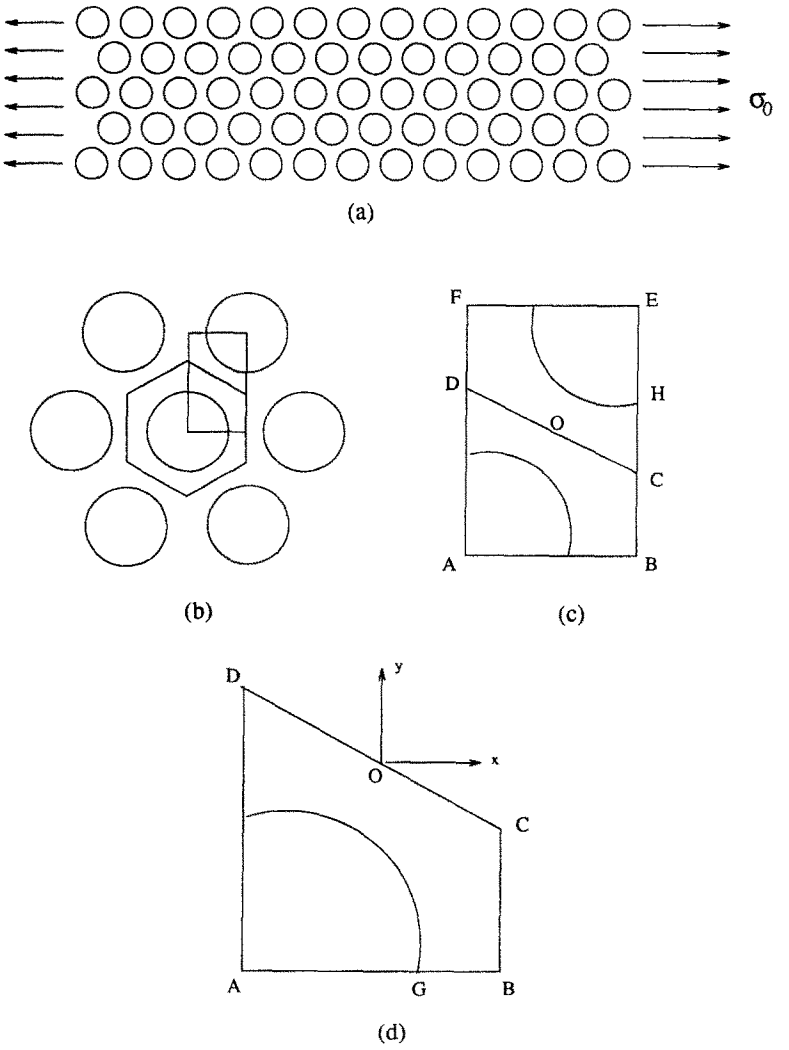

Fig. 1. (a) Hexagonal array subjected to far-field uniform tensile stress in CPD, (b) basic cell, (c) quarter region of basic cell, and (d) trapezoidal domain for numerical calculations.

$$\int_{BC+CO} \tau_1(s)\,ds = \tfrac{3}{4}b\sigma_0, \tag{5}$$

$$\int_{CD} \tau_2(s)\,ds = 0, \tag{6}$$

where u_i and τ_i, $i = 1, 2$ are the components of the displacement and traction vectors, respectively, and C_1 and C_2 are (as yet) unknown constants.

Interphase conditions, with respect to local polar co-ordinates r and θ, centered at A, are of the form (the outward normal to a region at a point on its boundary is taken to be positive)

$$\text{No contact:}\quad \tau_r^{(m)} = -\tau_r^{(f)} = -k_r(u_r^{(m)} - u_r^{(f)}) \quad \text{if } u_r^{(m)} > u_r^{(f)}, \tag{7}$$

$$\text{Contact:}\quad \tau_r^{(m)} = -\tau_r^{(f)}, \quad u_r^{(m)} = u_r^{(f)} \quad \text{if } u_r^{(m)} \not> u_r^{(f)}, \tag{8}$$

$$\tau_\theta^{(m)} = -\tau_\theta^{(f)} = -k_\theta(u_\theta^{(m)} - u_\theta^{(f)}), \tag{9}$$

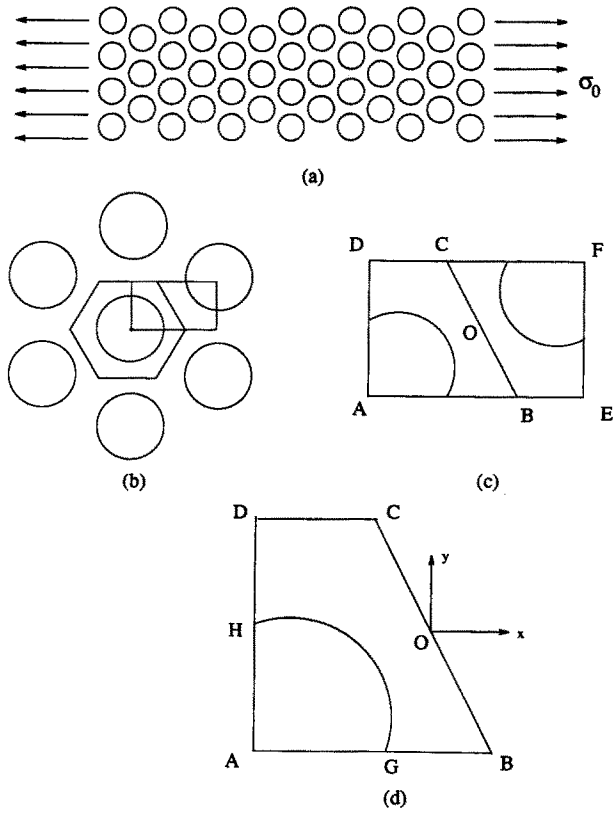

Fig. 2. (a) Hexagonal array subjected to far-field uniform tensile stress in mid-CPD, (b) basic cell, (c) quarter region of basic cell, and (d) trapezoidal domain for numerical calculations.

where the superscripts m and f refer to the matrix and the fiber, respectively, and k_r and k_θ are the stiffnesses of the interphase in the r and θ directions. Equation (7) refers to separation and (8) to contact between a point on the fiber and the corresponding point on the matrix.

3. INTEGRAL EQUATIONS FOR THE MECHANICS PROBLEM

Following Rizzo (1967), boundary integral equations are written separately for the matrix and the fiber in the trapezoidal region $ABCD$ of Fig. 1. For the matrix,

$$C_{ij}(P)u_j^{(m)}(P) = \int_{\partial B_1 U \partial B_2} [U_{ij}^{(m)}(P, Q)\tau_j^{(m)}(Q) - T_{ij}^{(m)}(P, Q)u_j^{(m)}(Q)]\,ds_Q,$$

$$P \in \partial B_1 U \partial B_2, \tag{10}$$

where $U_{ij}^{(m)}$ and $T_{ij}^{(m)}$ are the well-known Kelvin kernels for plane strain problems [see, for example, Mukherjee (1982)], for the matrix, and C_{ij} is the corner tensor. Also, P and Q are the source and field points, respectively, and $\partial B_1 = GB + BC + CD + DH$ and $\partial B_2 = HG$ in Fig. 1.

Similarly, for the fiber,

$$C_{ij}(P)u_j^{(f)}(P) = \int_{\partial B_2 U \partial B_3} [U_{ij}^{(f)}(P, Q)\tau_j^{(f)}(Q) - T_{ij}^{(f)}(P, Q)u_j^{(f)}(Q)]\,ds_Q,$$

$$P \in \partial B_2 U \partial B_3, \tag{11}$$

where $\partial B_3 = HA + AG$ in Fig. 1.

4. EQUATIONS FOR THE SENSITIVITY PROBLEM

The design variables here are the interphase stiffnesses k_r and k_θ. Sensitivity of a dependent variable ϕ with respect to k_r is denoted as ϕ^* and sensitivity with respect to k_θ is denoted as ϕ°, i.e.

$$\phi^* = \frac{\partial \phi}{\partial k_r}, \quad \phi^o = \frac{\partial \phi}{\partial k_\theta}. \tag{12}$$

Differentiating eqns (1)–(6) with respect to k_r, one gets,

$$AB: \quad \tau_1^* = 0, \quad u_2^* = C_2^*, \tag{13}$$

$$BC: \quad \tau_2^* = 0, \quad u_1^* = C_1^*/2, \tag{14}$$

$$DA: \quad \tau_2^* = 0, \quad u_1^* = -C_1^*/2, \tag{15}$$

$$DC: \quad \begin{cases} u_1^*(-x,-y) = -u_1^*(x,y), \\ u_2^*(-x,-y) = -u_2^*(x,y), \\ \tau_1^*(-x,-y) = \tau_1^*(x,y), \\ \tau_2^*(-x,-y) = \tau_2^*(x,y), \end{cases} \tag{16}$$

$$\int_{BC+CO} \tau_1^*(s)\,\mathrm{d}s = 0, \tag{17}$$

$$\int_{CD} \tau_2^*(s)\,\mathrm{d}s = 0. \tag{18}$$

Interphase sensitivity equations are obtained by differentiating eqns (7)–(9) with respect to k_r. These are

$$\text{No contact:} \quad \tau_r^{*(\mathrm{m})} = -\tau_r^{*(\mathrm{f})} = -k_r(u_r^{*(\mathrm{m})} - u_r^{*(\mathrm{f})}) - (u_r^{(\mathrm{m})} - u_r^{(\mathrm{f})}) \quad \text{if } u_r^{(\mathrm{m})} > u_r^{(\mathrm{f})}, \tag{19}$$

$$\text{Contact:} \quad \tau_r^{*(\mathrm{m})} = -\tau_r^{*(\mathrm{f})}, \quad u_r^{*(\mathrm{m})} = u_r^{*(\mathrm{f})} \quad \text{if } u_r^{(\mathrm{m})} \not> u_r^{(\mathrm{f})}, \tag{20}$$

$$\tau_\theta^{*(\mathrm{m})} = -\tau_\theta^{*(\mathrm{f})} = -k_\theta(u_\theta^{*(\mathrm{m})} - u_\theta^{*(\mathrm{f})}). \tag{21}$$

Finally, the boundary integral equations (10) and (11) must be differentiated with respect to k_r to give

$$C_{ij}(P)u_j^{*(\mathrm{m})}(P) = \int_{\partial B_1 U \partial B_2} [U_{ij}^{(\mathrm{m})}(P,Q)\tau_j^{*(\mathrm{m})}(Q) - T_{ij}^{(\mathrm{m})}(P,Q)u_j^{*(\mathrm{m})}(Q)]\,\mathrm{d}s_Q,$$

$$P \in \partial B_1 U \partial B_2, \tag{22}$$

$$C_{ij}(P)u_j^{*(\mathrm{f})}(P) = \int_{\partial B_2 U \partial B_3} [U_{ij}^{(\mathrm{f})}(P,Q)\tau_j^{*(\mathrm{f})}(Q) - T_{ij}^{(\mathrm{f})}(P,Q)u_j^{*(\mathrm{f})}(Q)]\,\mathrm{d}s_Q,$$

$$P \in \partial B_2 U \partial B_3. \tag{23}$$

It should be noted that the differentiations are implicit as well as explicit with respect to k_r. Also, if shape sensitivities (e.g. with respect to volume fraction) are considered, then one must also differentiate the kernels U_{ij} and T_{ij} and the length element $\mathrm{d}s$ with respect to

appropriate parameters that define the boundary of the body. Such issues are discussed, in detail, in Zhang and Mukherjee (1991).

Similar equations can easily be derived for sensitivities with respect to k_θ. Equations (13)–(18) and (22), (23) remain unchanged except for the * being replaced by the °. Interphase equations (19)–(21) must now be replaced by

$$\text{No contact:} \quad \tau_r^{\circ(\mathrm{m})} = -\tau_r^{\circ(\mathrm{f})} = -k_r(u_r^{\circ(\mathrm{m})} - u_r^{\circ(f)}) \quad \text{if } u_r^{(\mathrm{m})} > u_r^{(\mathrm{f})}, \tag{24}$$

$$\text{Contact:} \quad \tau_r^{\circ(\mathrm{m})} = -\tau_r^{\circ(\mathrm{f})}, \quad u_r^{\circ(\mathrm{m})} = u_r^{\circ(f)} \quad \text{if } u_r^{(\mathrm{m})} \not> u_r^{(\mathrm{f})}, \tag{25}$$

$$\tau_\theta^{\circ(\mathrm{m})} = -\tau_\theta^{\circ(f)} = -k_\theta(u_\theta^{\circ(\mathrm{m})} - u_\theta^{\circ(\mathrm{f})}) - (u_\theta^{(\mathrm{m})} - u_\theta^{(\mathrm{f})}). \tag{26}$$

5. NUMERICAL IMPLEMENTATION

Numerical implementation of the BEM equations, using quadratic isoparametric boundary elements, is carried out in standard fashion [see, for example, Mukherjee (1982) and Brebbia and Dominguez (1992)]. The latter book (Brebbia and Dominguez, 1992) also lists computer routines for such numerical implementations involving standard elasticity problems. For the mechanics problem, each of the equations (10) and (11) are suitably discretized. The boundary interphase equations (1)–(9) are employed. Corners on the trapezoid in the two regions (points A, G, B, C, D and H in Fig. 1) are modeled by putting double nodes at each corner.

All integrations are carried out numerically. The logarithmically singular kernel U_{ij} is integrated by log weighted Gaussian integration. The $O(1/r)$ singular kernel, T_{ij} is integrated indirectly by using rigid body modes and writing the integral over a singular element (together with the corner tensor, C_{ij}), in terms of regular integrals of T_{ij} over the test of the boundary [see, for example, Mukherjee (1982) and Brebbia and Dominguez (1992)].

An additional complication arises from the contact equations (7)–(9). Initially, eqn (7) is assumed to apply at all interphase nodes. If $\sigma_{rr}^{(\mathrm{m})} = \sigma_{rr}^{(\mathrm{f})}$ at any interphase node(s) is negative, eqn (8) replaces eqn (7) at those nodes and the calculation is repeated. This procedure finally converges to the correct solution. The sensitivity calculations are carried out in a manner entirely analogous to the mechanics problem.

For the numerical calculations, the material properties chosen are (Achenbach and Zhu, 1990)

$$\mu^{(\mathrm{m})} = 14.4 \text{ Msi} \quad (9.79 \times 10^4 \text{ MPa}), \quad \nu^{(\mathrm{m})} = 0.22,$$
$$\mu^{(\mathrm{f})} = 30.0 \text{ Msi} \quad (2.07 \times 10^5 \text{ MPa}), \quad \nu^{(\mathrm{f})} = 0.30,$$

where μ and ν are the shear modulus and Poisson's ratio, of each material, respectively. The above values of the physical constants are typical of metal fiber-ceramic composites, for example, copper alloy fibers in a tungsten carbide matrix (Weeton *et al.*, 1987).

Assuming a fiber volume fraction $V_\mathrm{f} = 0.4$, one gets,

$$\frac{b}{a} = \left(\frac{5\pi}{3\sqrt{3}}\right)^{1/2} = 1.7387.$$

The nondimensional tractions, stresses and interphase stiffnesses are defined as,

$$\hat{\sigma}_{ij} = \frac{\sigma_{ij}}{\sigma_\mathrm{o}}, \quad \hat{\tau}_i = \frac{\tau_i}{\sigma_\mathrm{o}}, \quad \hat{k}_r = \frac{ak_r}{\mu^{(\mathrm{m})}}, \quad \hat{k}_\theta = \frac{ak_\theta}{\mu^{(\mathrm{m})}},$$

so that the nondimensional sensitivities are

$$\frac{\partial \hat{\tau}_i}{\partial \hat{k}_r} = \left(\frac{\mu^{(m)}}{a\sigma_0}\right)\tau_i^*, \quad \frac{\partial \hat{\tau}_i}{\partial \hat{k}_\theta} = \left(\frac{\mu^{(m)}}{a\sigma_0}\right)\tau_i^0$$

and

$$\frac{\partial \hat{\sigma}_{ij}}{\partial \hat{k}_r} = \left(\frac{\mu^{(m)}}{a\sigma_0}\right)\sigma_{ij}^*, \quad \frac{\partial \hat{\sigma}_{ij}}{\partial \hat{k}_\theta} = \left(\frac{\mu^{(m)}}{a\sigma_0}\right)\sigma_{ij}^0.$$

The interphase stiffnesses k_r and k_θ depend upon the shear and bulk moduli of the interphase material and the thickness of the interphase. There is considerable uncertainty, at present, in these values for physical composite systems. A nominal value of $\hat{k}_r = \hat{k}_\theta = 1/14.4 = 0.0694$ has been used in some of the calculations presented in the next section of this paper. Different values have been used for the results presented in the section on jump discontinuities in sensitivities. These values are given in the appropriate subsection.

6. NUMERICAL RESULTS

6.1. *Sensitivities of fiber tractions at the interface*

The first example is concerned with the calculations of sensitivities of tractions $\tau_r^{(m)}$ and $\tau_\theta^{(m)}$ with respect to the interphase stiffnesses k_r and k_θ. These base values are $\hat{k}_r = \hat{k}_\theta = 0.0694$.

Results for $\partial \hat{\tau}_r/\partial \hat{k}_r$, as a function of position (angle) around a quarter of the fiber (anticlockwise positive) for the CPD cases, are given in Table 1. Also given are the results from the finite difference of two BEM solutions with $\Delta \hat{k}_r = 0.01\hat{k}_r$ and $\Delta \hat{k}_r = 0.001\hat{k}_r$, respectively, and the state of contact of each interphase node with a 0 indicating no contact and 1 indicating contact. The sensitivity results are seen to agree very well in all cases.

Figures 3–6 display the quantities $\partial \hat{\tau}_r/\partial \hat{k}_r$, $\partial \hat{\tau}_\theta/\partial \hat{k}_r$, $\partial \hat{\tau}_r/\partial \hat{k}_\theta$, $\partial \hat{\tau}_\theta/\partial \hat{k}_\theta$, respectively, for the CPD case, as a function of the angle measured around a quarter of the fiber, while Figs 7–10 display the same quantities for the mid-CPD case. The base values are the same as those for Table 1. Again, the BEM and FDM (with 1% perturbation of the appropriate stiffness) results agree perfectly within plotting accuracy. The state of each boundary node with respect to contact is also shown in these figures.

An interesting result is that, for all the cases involving τ_r (Figs 3, 5, 7 and 9), the sensitivities, in general, are small and relatively uniform at points in the interphase where the matrix and the fiber are not in contact, compared to those that are in contact. This result is somewhat surprising because k_r is inactive at points of contact. Of course, the results at contact points are affected by changes in k_r at other points.

6.2. *Jumps in traction sensitivities*

A very interesting question is related to the behavior of traction sensitivities at values of stiffnesses where the interphase configuration (in terms of points in contact) changes due

Table 1. Sensitivities of $\hat{\tau}_r$ with respect to $\hat{k}_r$ for the CPD case with base values of $\hat{k}_r$ and $\hat{k}_\theta$ equal to 0.0694

Angle	Contact condition	BEM sensitivities	1% FDM sensitivities	0.1% FDM sensitivities
0	0	−0.7816	−0.7891	−0.7838
10	0	−0.7449	−0.7446	−0.7446
20	0	−0.7271	−0.7258	−0.7272
30	0	−0.6473	−0.6451	−0.6466
40	0	−0.3686	−0.3686	−0.3686
50	0	−0.7105	−0.7102	−0.7113
60	0	−0.3908	−0.3907	−0.3917
70	1	1.7986	1.8000	1.7986
80	1	0.1166	0.1166	0.1166
88	1	−1.9858	−1.9872	−1.9872
90	1	1.2256	1.2384	1.2384

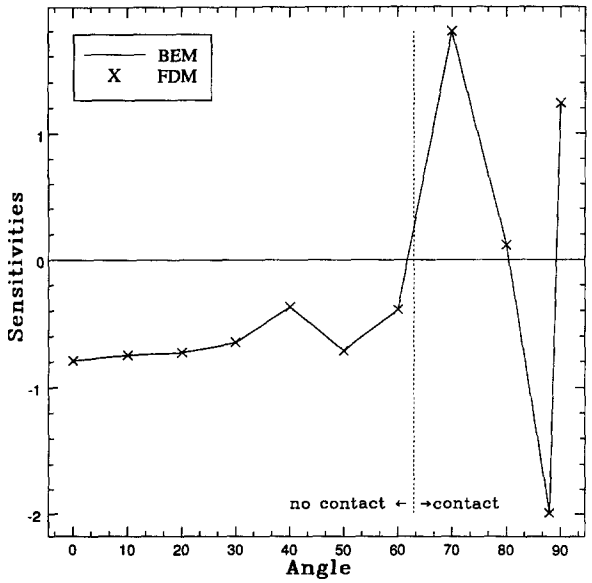

Fig. 3. Sensitivities of $\hat{t}_r$ with respect to $\hat{k}_r$ for the CPD case with base values of $\hat{k}_r$ and k_θ equal to 0.0694.

to a small change in the stiffness. In such a situation, the sensitivity at an interphase point might become discontinuous. Such a situation is schematically depicted in Fig. 11. Let P be such a point of sensitivity discontinuity and P_1 and P_2 be neighboring points on either side of it.

A numerical calculation has been carried out for $\hat{k}_{r1} = 0.5378$ at point P_1 and $\hat{k}_{r2} = (1.01)(0.5378) = 0.5432$ at P_2. The value of $\hat{k}_\theta$ has been kept fixed at 0.6944. The following results have been obtained:

(1) The sensitivities $\partial \hat{t}_r / \partial \hat{k}_r$, from the BEM program, at points P_1 and P_2.

(2) Results from the backward and forward FDMs, with a 1% perturbation in k_r, with the base value equal to k_{r1}.

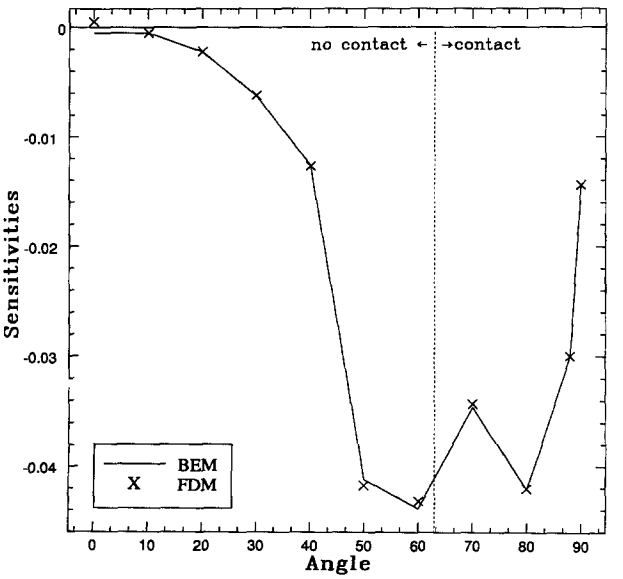

Fig. 4. Sensitivities of $\hat{t}_\theta$ with respect to $\hat{k}_r$ for the CPD case with base values of $\hat{k}_r$ and k_θ equal to 0.0694.

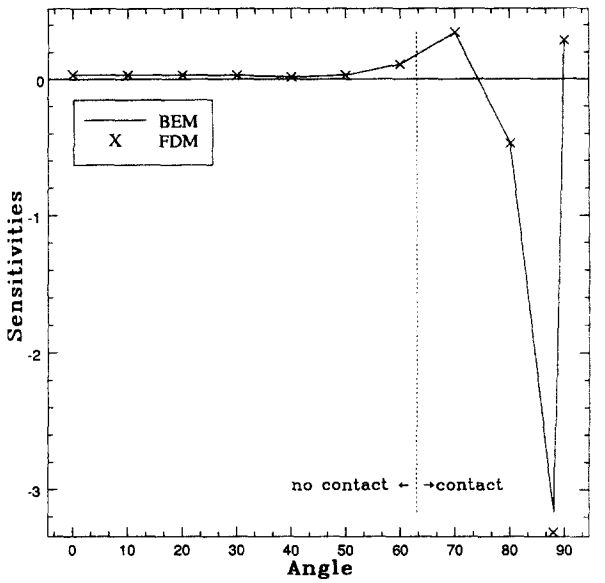

Fig. 5. Sensitivities of $\hat{\tau}_r$ with respect to $\hat{k}_\theta$ for the CPD case with base values of $\hat{k}_r$ and k_θ equal to 0.0694.

(3) Same as case (2) but with base value of k_{r2}.

The results are shown in Tables 2 and 3, for base values k_{r1} and k_{r2}, respectively. The BEM results show the expected jump in sensitivities due to the node at $\theta = 90°$, changing from no contact at k_{r1} to contact at k_{r2}. The jumps are larger at points near the node at $\theta = 90°$ than those at points far away from it. As expected, the backward FDM works fine at k_{r1}, while the forward FDM, oblivious to the change in interphase configuration, gives completely erroneous results. The reverse is true at k_{r2} as seen from the Table 3 (see also Fig. 11). This example shows that while the BEM results, based on analytical differentiation of the governing equations, are reliable, the FDM results can be totally wrong if attention is not paid to a change in the system configuration due to a perturbation in a stiffness value.

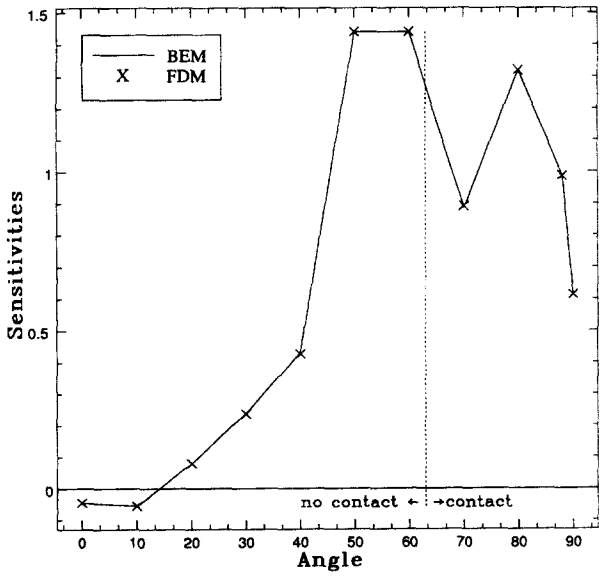

Fig. 6. Sensitivities of $\hat{\tau}_\theta$ with respect to $\hat{k}_\theta$ for the CPD case with base values of $\hat{k}_r$ and k_θ equal to 0.0694.

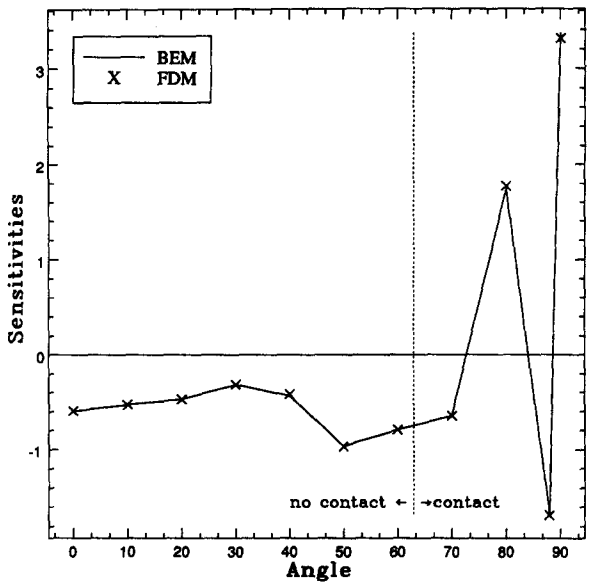

Fig. 7. Sensitivities of $\hat{\tau}_r$ with respect to $\hat{k}_r$ for the mid-CPD case with base values of $\hat{k}_r$ and k_θ equal to 0.0694.

6.3. *Sensitivities of tangential stresses in the matrix at an interphase*

Tangential stresses in the matrix, at an interface are very important quantities, since large tensile tangential stresses can cause fracture of the matrix. The sensitivities of these stresses with respect to k_r and k_θ, in dimensionless form (i.e. $\partial\hat{\sigma}_{\theta\theta}\backslash\partial\hat{k}_r$ and $\partial\hat{\sigma}_{\theta\theta}\backslash\partial\hat{k}_\theta$), as functions of θ, are shown in Figs 12 and 13, respectively. These results are for the CPD case. The base values of the geometrical and physical quantities are the same as those used for Figs 3–10. Again, the BEM results agree well with those obtained by the finite differences of the BEM solutions.

Figures 3, 4 and 12 show the sensitivities of the three components of the stress, at the interface, with respect to k_r, while Figs 5, 6 and 13 show the sensitivities of the same quantities with respect to k_θ. A comparison of Figs 3, 4 and 12 shows that the radial and

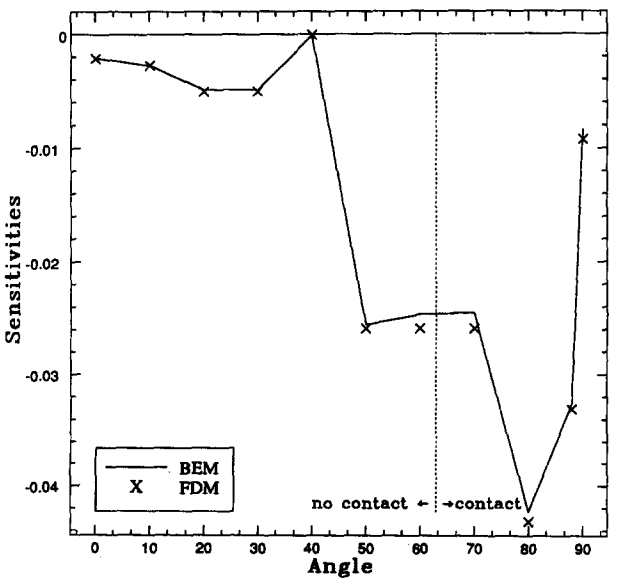

Fig. 8. Sensitivities of $\hat{\tau}_\theta$ with respect to $\hat{k}_r$ for the mid-CPD case with base values of $\hat{k}_r$ and k_θ equal to 0.0694.

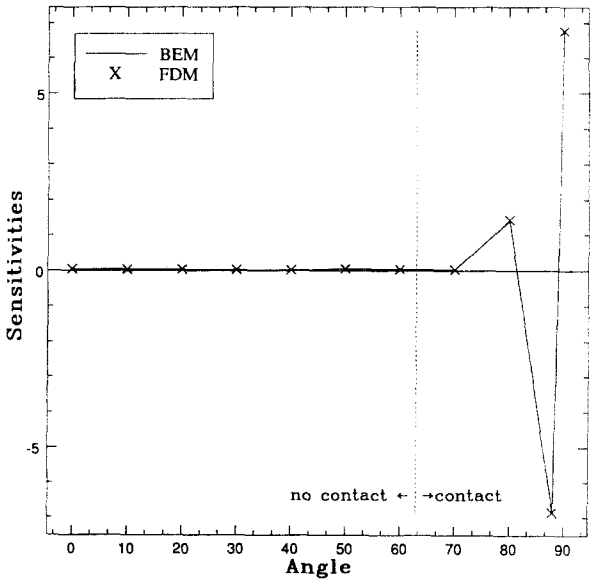

Fig. 9. Sensitivities of $\hat{\tau}_r$ with respect to $\hat{k}_\theta$ for the mid-CPD case with base values of $\hat{k}_r$ and k_θ equal to 0.0694.

tangential stresses are more sensitive to k_r as compared to the shearing stress $\sigma_{r\theta}$. Similarly, a comparison of Figs 5, 6 and 13 shows that σ_{rr} and $\sigma_{\theta\theta}$ are most sensitive to k_θ, although the maxima are attained at different locations around the fiber. As mentioned before, the sensitivities of $\sigma_{\theta\theta}$ are of most concern in design because large tensile hoop stresses could lead to matrix failure.

6.4. *Optimization of interphase stiffnesses*

Standard mechanics analysis, together with sensitivity analysis, is used in conjunction with nonlinear programming [in this case sequential quadratic programming—Schittkowski (1986)] to carry out optimal design of interphase stiffnesses. As stated before, the IMSL subroutine N0ONF is used to perform the optimization. The necessary gradients required

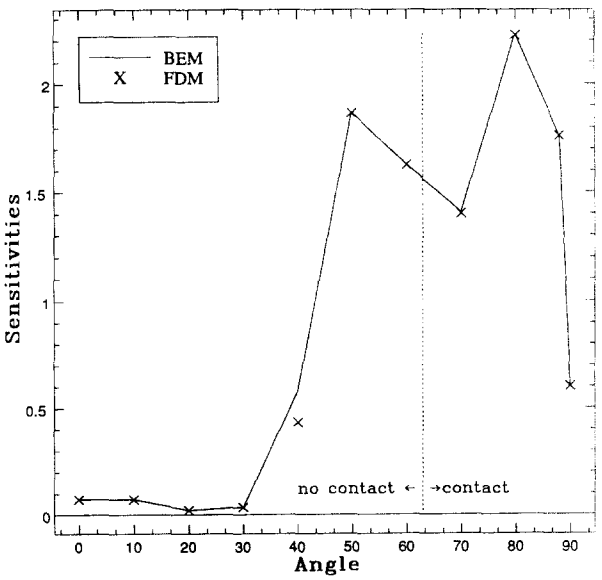

Fig. 10. Sensitivities of $\hat{\tau}_\theta$ with respect to $\hat{k}_\theta$ for the mid-CPD case with base values of $\hat{k}_r$ and k_θ equal to 0.0694.

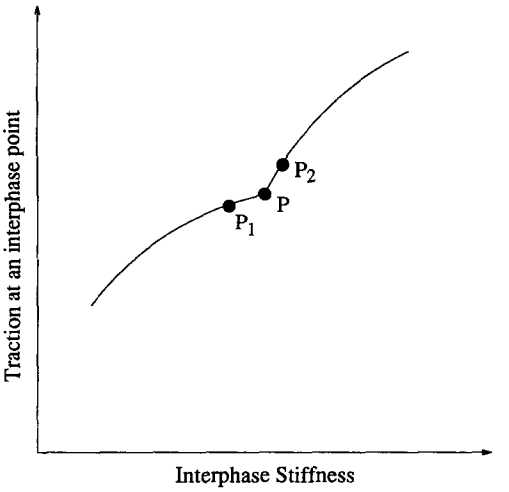

Fig. 11. Schematic representation of dependence of interphase traction on interphase stiffness. The interphase configuration undergoes a change at point P.

for every iteration by this subroutine are provided by the sensitivity analysis. The overall approach used in this case is illustrated in the flowchart shown in Fig. 14.

The central idea in this phase of the work is to design interphase stiffnesses to minimize the possibility of failure of the composite subjected to a prescribed loading. Failure can occur at the interphase (debonding), in the matrix or in a fiber. To incorporate such an optimization criterion, one can choose among various failure criteria involving quantities

Table 2. Sensitivities of $\hat{t}_r$ with respect to $\hat{k}_r$ for the CPD case with $\hat{k}_r = 0.5378$ and $\hat{k}_\theta = 0.6944$

Angle	Contact condition	BEM sensitivities	Backward 1% FDM sensitivities	Forward 0.1% FDM sensitivities
0	0	−0.4260	−0.4269	0.4381
10	0	−0.3788	−0.3796	0.5071
20	0	−0.3581	−0.3589	0.6174
30	0	−0.3056	−0.3063	0.7496
40	0	−0.1540	−0.1545	0.5441
50	0	−0.3365	−0.3376	−0.0937
60	0	−0.2119	−0.2129	−1.0095
70	0	−0.1303	−0.1311	−1.5165
80	1	0.7207	0.7232	−43.6641
88	1	−0.7238	−0.7250	−163.5637
90	1	0.5259	0.5277	910.3122

Table 3. Sensitivities of $\hat{t}_r$ with respect to $\hat{k}_r$ for the CPD case with $\hat{k}_r = 0.5432$ and $\hat{k}_\theta = 0.0694$

Angle	Contact condition	BEM sensitivities	Backward 1% FDM sensitivities	Forward 0.1% FDM sensitivities
0	0	−0.4183	0.4380	−0.4177
10	0	−0.3710	0.5071	−0.3703
20	0	−0.3496	0.6173	−0.3587
30	0	−0.2963	0.7496	−0.2955
40	0	−0.1475	0.5441	−0.1469
50	0	−0.3332	−0.0937	−0.3321
60	0	−0.2172	−1.0095	−0.2161
70	0	−0.1410	−1.5165	−0.1403
80	1	0.7478	−43.6641	0.7479
88	1	−0.5933	−163.5637	0.5928
90	0	−0.2342	910.3122	−0.2342

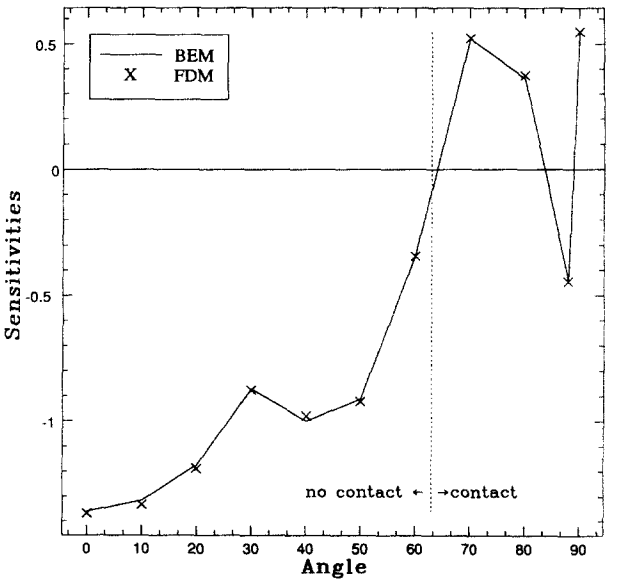

Fig. 12. Sensitivities of $\hat{\sigma}_{\theta\theta}$ with respect to $\hat{k}_r$ for the CPD case with base values of $\hat{k}_r$ and k_θ equal to 0.0694.

such as strain energy, distortion energy, maximum principal tensile stress, maximum shearing stress, etc. The precise choice of such a criterion, however is quite subjective, especially in view of the somewhat uncertain nature of the interphase. It is important to emphasize, however, that the optimization approach described here is general and would work, in principle, for any choice of a failure criterion.

A somewhat simplistic view is taken in the illustrative examples that follow. It is clear that large values of (tensile) radial or shearing stresses at an interphase can cause debonding failure of the interphase while large tensile hoop stresses in a ceramic matrix could lead to its cracking and eventually failure. Whether failure occurs in the matrix, fiber or the interphase depends upon many factors including the loading and relative strengths of the different components of a composite. With this in view, one can choose an objective function of the type

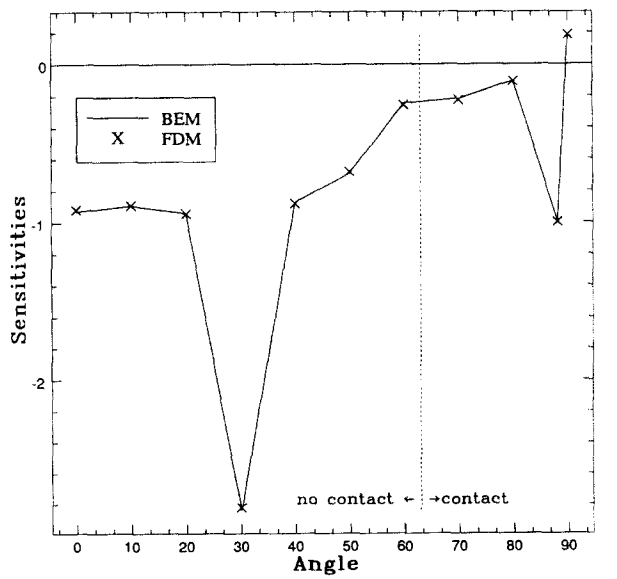

Fig. 13. Sensitivities of $\hat{\sigma}_{\theta\theta}$ with respect to $\hat{k}_\theta$ for the CPD case with base values of $\hat{k}_r$ and k_θ equal to 0.0694.

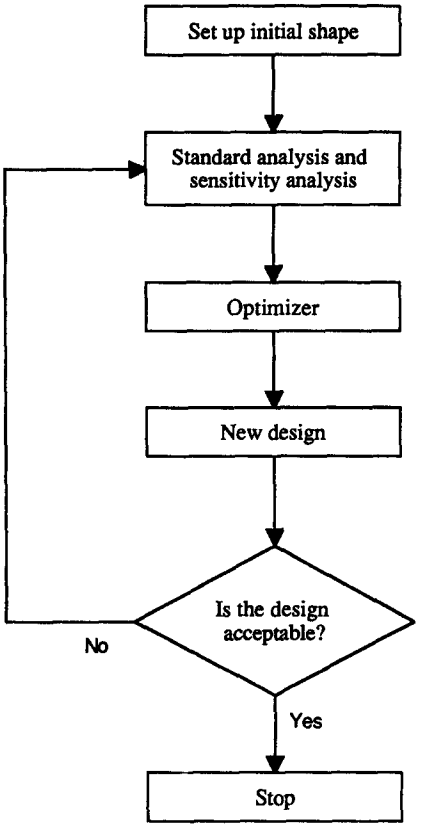

Fig. 14. Optimal design algorithm.

$$\phi = \max\,(\alpha\sigma_{rr} + \beta\sigma_{\theta\theta}), \tag{27}$$

with $\sigma_{rr} \geqslant 0$, $\sigma_{\theta\theta} \geqslant 0$, which is the maximum value of a linear combination of, say σ_{rr} in the interphase and $\sigma_{\theta\theta}$ in the matrix at an interface, with the weightings α and β reflecting the relative strengths of the interphase and matrix materials, respectively. If, for example, the interphase were very weak relative to the matrix, one would choose $\alpha = 1$ and $\beta = 0$ in eqn (27).

Two illustrative examples for the CPD case are described below.

Example 1: Minimize (ϕ) where $\phi = \max.\,(\hat{\sigma}_{rr})$ in the interphase, subject to the constraints

$$\begin{aligned} &(1)\ \hat{\sigma}_{rr} \geqslant 0,\\ &(2)\ 0.694 \leqslant \hat{k}_r \leqslant 34.72,\\ &(3)\ 0.694 \leqslant \hat{k}_\theta \leqslant 34.72, \end{aligned}$$

where $\hat{k}_r$ and $\hat{k}_\theta$ are the design variables. The above range for $\hat{k}_r$ and $\hat{k}_\theta$ corresponds to minimum and maximum values of 10 Msi (6.80×10^4 MPa) and 50 Msi (34×10^4 MPa), respectively.

The results of successive iterations, from the optimization procedure, are shown in Table 4. It is seen that the optimal values of the design variables for this problem are, as expected, the minimum values for $\hat{k}_r$ and $\hat{k}_\theta$ within the specified range of these variables.

Example 2: Minimize (ϕ) where $\phi = \max.\,(\hat{\sigma}_{rr} + \hat{\sigma}_{\theta\theta})$, the maximum value of ϕ being taken over the interface. Here, σ_{rr} is the nondimensionalized stress in the interphase while $\hat{\sigma}_{\theta\theta}$ is the hoop stress in the matrix at the interface. The constraints chosen here are

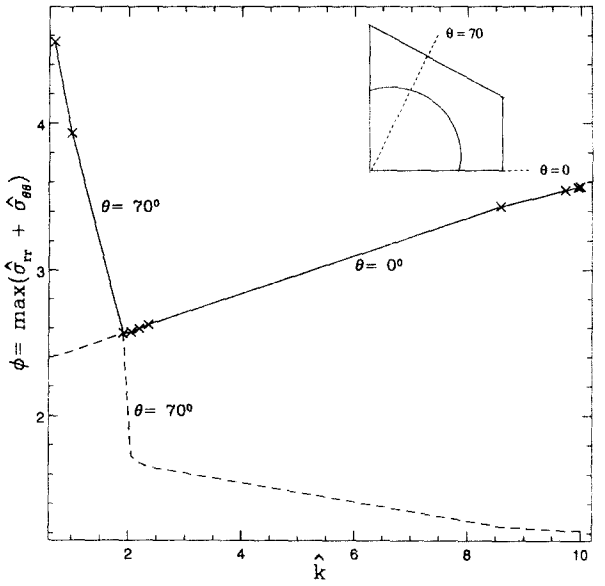

Fig. 15. $\phi = \max(\hat{\sigma}_{rr} + \hat{\sigma}_{\theta\theta})$ (Example 2), as a function of $\hat{k}$ (solid line). Values of successive iterations are shown with crosses.

(1) $\hat{\sigma}_{rr} \geqslant 0$,

(2) $\hat{\sigma}_{\theta\theta} \geqslant 0$,

(3) $\hat{k}_r = \hat{k}_\theta = \hat{k}$,

(4) $0.694 \leqslant \hat{k} \leqslant 34.72$.

The third constraint is chosen here to simplify the analysis, but can be relaxed if desired.

Figure 15 shows ϕ as a function of $\hat{k}$. For $0.694 \leqslant \hat{k} \leqslant \hat{k}_{\text{opt}}$, the maximum value of $\hat{\sigma}_{rr} + \hat{\sigma}_{\theta\theta}$ occurs at the angular location $\theta = 70°$, while, for $\hat{k}_{\text{opt}} \leqslant \hat{k} \leqslant 34.72$, the location of the maximum value shifts to $\theta = 0°$. The optimal value of $\hat{k}$ in this case, is 1.908 which occurs when $\phi_{\theta=0°}$ equals $\phi_{\theta=70°}$. Values of ϕ for successive iterations from the optimizer

Table 4. Successive iterations for the optimization problem $\phi = \max(\hat{\sigma}_{rr})$ in the interphase

Iteration	$\hat{k}_r$	$\hat{k}_\theta$	ϕ
1	3.000	2.000	0.6713
2	0.694	1.113	0.4061
3	2.663	1.870	0.5935
4	0.694	0.694	0.3432

Table 5. Successive iterations for the optimization problem $\phi = \max(\hat{\sigma}_{rr} + \hat{\sigma}_{\theta\theta})$ on the interface

Iteration	$\hat{k}$	ϕ
1	10.000	3.5671
2	9.955	3.5630
3	9.729	3.5425
4	8.581	3.4328
5	2.359	2.6253
6	0.694	4.5569
7	2.193	2.5984
8	0.694	4.5569
9	2.043	2.5742
10	0.694	4.5569
11	1.908	2.5659

are shown in Table 5. In this case, 11 iterations are needed to converge to the optimal value of $\hat{k}$.

7. CONCLUSIONS

An important question related to the design of composite materials has been raised in this paper—is it possible to tailor the composite interphase properties such as strength or stiffness in order to achieve desired objectives? A first crucial step towards this objective is the efficient and accurate calculation of the appropriate design sensitivities. A calculation of sensitivities of stresses at the interphase, with respect to interphase stiffnesses, has been carried out here. It is shown that the DDA of the governing BEM equations of the problem provide an accurate and efficient way to carry out these calculations. The FDM approach, while easier to employ, can give totally erroneous results in cases where a sensitivity suffers a jump discontinuity.

Next, the use of these sensitivities in an optimization procedure is demonstrated through two illustrative examples. Optimal values of interphase stiffness, to minimize the possibility of failure of a composite under prescribed loading, are obtained in these examples. Of future interest is the calculation of sensitivities of residual stresses in a matrix material which is modeled as elasto-plastic. Research along these lines is currently in progress.

Acknowledgements—This research has been supported by NSF grant number MSS-8922185 to Cornell University and the University of Arizona. All computing for this research has been performed at the Cornell National Supercomputer Facility.

REFERENCES

Aboudi, J. (1987). Damage in composites modelling of imperfect bonding. *Compos. Sci. Technol.* **28,** 103–128.

Achenbach, J. D. and Zhu, H. (1989). Effect of interfacial zone on mechanical behavior and failure of fiber-reinforced composites. *J. Mech. Phys. Solids* **37,** 381–393.

Achenbach, J. D. and Zhu, H. (1990). Effect of interphases on micro and macromechanical behavior of hexagonal-array fiber composites. *ASME J. Appl. Mech.* **57,** 956–963.

Adams, D. F. (1987). A micromechanical analysis of the influence of the interface on the performance of polymer matrix composites. *J. Reinforced Plastics Compos.* **6,** 66–87.

Aithal, R., Saigal, S. and Mukherjee, S. (1991). Three dimensional boundary element implicit-differentiation formulation for design sensitivity analysis. *Math. Comput. Model.* **15,** 1–10.

Barone, M. R. and Yang, R. J. (1988). Boundary integral equations for recovery of design sensitivities in shape optimization. *AIAA Jl* **26,** 589–594.

Barone, M. R. and Yang, R. J. (1989). A boundary element approach for recovery of shape sensitivities in three-dimensional elastic solids. *Comput. Meth. Appl. Mech. Engng* **17,** 69–82.

Benveniste, Y. (1985). The effective mechanical behavior of composite materials with imperfect contact between the constituents. *Mech. Mater.* **4,** 197–208.

Benveniste, Y., Dvorak, G. J. and Chen, T. (1989). Stress fields in composites with coated inclusions. *Mech. Mater.* **7,** 305–317.

Brebbia, C. A. and Dominguez, J. (1992). *Boundary Elements: An Introductory Course.* McGraw-Hill, Southampton, Boston.

Broutman, L. J. and Agarwal, B. D. (1974). A theoretical study of the effect of an interfacial layer on the properties of composites. *Polymer Engng Sci.* **14,** 581–588.

Choi, J. H. and Choi, K. K. (1990). Direct differentiation method for shape design sensitivity analysis using boundary integration formulation. *Comput. Struct.* **34,** 499–508.

Haftka, R. T., Gurdal, Z. and Kamat, M. P. (1990). *Elements of Structural Optimization.* Kluwer Academic Publishers, Dordrecht, The Netherlands.

Hashin, Z. (1990). Thermoelastic properties of fiber composite with imperfect interface. *Mech. Mater.* **8,** 333–348.

Hashin, Z. (1991). Composite materials with viscoelastic interphase: Creep and relaxation. *Mech. Mater.* **11,** 135–148.

Jasiuk, I. and Tong, Y. (1989). The effect of interface on the elastic stiffness of composites. In *Mechanics of Composite Materials and Structures* (Edited by J. N. Reddy and J. L. Teply), ASME AMD-Vol. 100, pp. 49–54.

Kane, J. H. and Saigal, S. (1988). Design sensitivity analysis of solids using BEM. *ASCE J. Engng Mech.* **114,** 1703–1722.

Lene, F. and Leguillon, D. (1982). Homogenized constitutive law for a partially cohesive composite material. *Int. J. Solids Structures* **18,** 443–458.

Mauerer, F. H. J., Sinha, R. and Jain, R. K. (1986). On the elastic moduli of particulate composites: Interlayer versus molecular model. In *Composites Interfaces* (Edited by H. Ishada and J. L. Koenig), pp. 367–374. North-Holland, New York.

Mikata, Y. and Taya, M. (1985a). Stress field in and around a coated short fiber in an infinite matrix subjective to uniaxial and biaxial loadings. *ASME J. Appl. Mech.* **52,** 19–26.

Mikata, Y. and Taya, M. (1985b). Stress field in a coated continuous fiber composite subjected to thermo-mechanical loadings. *J. Compos. Mater.* **19,** 554–578.

Mukherjee, S. (1982). *Boundary Element Methods in Creep and Fracture.* Elsevier, London.

Ochiai, S. and Osamura, K. (1987). A computer simulation of strength of metal matrix composites with a reaction layer at the interface. *Metall. Trans.* **18(A),** 673–679.

Rice, J. R. and Mukherjee, S. (1990). Design sensitivity coefficients for axisymmetric elasticity problems by boundary element methods. *Engng Anal. with Boundary Elements* **7,** 13–20.

Rizzo, F. J. (1967). An integral equation approach to boundary value problems of classical elastostatics. *Q. Appl. Math.* **25,** 83–95.

Saigal, S., Borggaard, J. T. and Kane, J. H. (1989). Boundary element implicit differentiation equations for design sensitivities of axisymmetric structures. *Int. J. Solids Structures* **25,** 527–538.

Schittkowski, K. (1986). NLPQL: A Fortran subroutine solving constrained nonlinear programming problems. *Annals Oper. Res.* **5,** 485–500.

Shieu, F. S., Raj, R. and Sass, S. L. (1990). Control of the mechanical properties of metal-ceramic interfaces through interfacial reactions. *Acta Metall. Mater.* **38,** 2215–2224.

Sideridis, E. (1988). The in-plane shear modulus of fiber reinforced composites as defined by the concept of interphase. *Compos. Sci. Technol.* **31,** 35–53.

Stief, P. and Hoysan, S. F. (1987). An energy method for calculating the stiffness of aligned short-fiber composites. *Mech. Mater.* **6,** 197–210.

Theocaris, P. S., Sideridis, E. P. and Papanicolaou, G. C. (1985). The elastic longitudinal modulus and Poisson's ratio of fiber composites. *J. Reinforced Plastics and Compos.* **4,** 396–418.

Vanderplaats, G. N. (1985). *ADS: A FORTRAN Program for Automated Design Synthesis.* Engineering Design Optimization Inc., Santa Barbara, CA.

Walpole, L. J. (1978). A coated inclusion in an elastic medium. *Math. Proc. Camb. Phil. Soc.* **83,** 495–506.

Weeton, J. W., Peters, D. M. and Thomas, K. L. (1987). *Engineers' Guide to Composite Materials.* American Society for Metals, Metals Park, OH.

Wei, X., Leu, L. J., Chandra, A. and Mukherjee, S. (1993). Shape optimization in elasticity and viscoplasticity (submitted for publication).

Zhang, Q. and Mukherjee, S. (1991). Design sensitivity coefficients for linear elastic bodies with zones and corners by the derivative boundary element method. *Int. J. Solids Structures* **27,** 983–998.

Zhang, Q., Mukherjee, S. and Chandra, A. (1992a). Design sensitivity coefficients for elasto-viscoplastic problems by boundary element methods. *Int. J. Num. Meth. Engng* **34,** 947–966.

Zhang, Q., Mukherjee, S. and Chandra, A. (1992b). Shape design sensitivity analysis for geometrically and materially nonlinear problems by the boundary element method. *Int. J. Solids Structures* **29,** 2503–2525.

Zywicz, E. (1986). Local stress and deformation due to fabrication and transverse loading in an ideal continuously reinforced graphite/aluminum metal matrix composite. M.Sc. Thesis, Department of Mechanical Engineering, MIT.